Debiasing of position estimations of UWB-based TDoA indoor positioning system

Paolo Grasso
Autonomous Vehicles & Artificial Intelligence Laboratory
Research Institute for Future Transport and Cities
Coventry University
Coventry, UK
grassop@coventry.ac.uk

Mauro S. Innocente
Autonomous Vehicles & Artificial Intelligence Laboratory
Research Institute for Future Transport and Cities
Coventry University
Coventry, UK
Mauro.S.Innocente@coventry.ac.uk

https://doi.org/10.31256/Ua2Vp3X

***Abstract*—When localising an object in a confined environment using an indoor positioning system (IPS) based on ultra-wideband (UWB) technology and an asynchronous time difference of arrival (TDoA) algorithm, systematic errors do occur. Theoretical estimation of these errors can be very hard to make. This study introduces a novel filtering algorithm for reducing the bias of position estimations, therefore increasing their accuracy. The problem is tackled for a two-dimensional IPS by formulating a *debiasing filter* using statistics of real data. Generalisation to the three-dimensional case should be straightforward.**

***Index Terms*—indoor positioning system (IPS), accuracy, bias, precision, time difference of arrival (TDoA), ultra-wideband (UWB)**

I. Introduction

In robotics and autonomy, positioning systems constitute a remarkably important technology. A variety of systems exist, which are aimed at different applications and make use of different algorithms (e.g. Time Difference of Arrival (TDoA) or Two Way Ranging) and different forms of energy (e.g. electromagnetic or sound waves). For example, Global Navigation Satellite Systems (GNSSs) are appropriate for efficient outdoor long-range positioning, while Indoor Positioning Systems (IPS) based on ultra-wideband (UWB) technology present crucial advantages in indoor spaces, namely high accuracy and the ability to penetrate obstacles [3]. It is important to emphasise that UWB positioning constitutes one of the most accurate and promising technologies for IPSs, arguably the best choice at present [3], [4]. A major drawback is given by its susceptibility to interferences, which may be caused by metallic materials and/or by systems working on similar frequencies.

This work builds on a previous study on the signal and geometrical properties of a general IPS [11]. In that study, the unbiased Cramér–Rao Lower Bound (CRLB) analysis for the reference IPS estimated that the precision inside the convex hull defined by the anchors was within ± 3 cm whereas the bias could not be assessed theoretically. Furthermore, an analysis based on [5]–[9] was performed in order to define the localisation boundary – i.e. the bifurcation envelope. Using the available IPS, this work aims to assess if the theoretical prediction of precision in [11] is correct and to estimate the order of magnitude of the bias. These data are subsequently used for the development of a debiasing filter aimed at increasing the accuracy of the position estimations. The state of the art of currently used IPS is the Extended Kalman Filter (EKF) developed by Mueller et al. [1], [2]. However, there are systematic errors that the EKF does not deal with, as observed in the experiments and acknowledged in [1]. The proposed debiasing filter is an attempt to find a solution to this problem.

II. Design of experiment on IPS

The purpose of the IPS under study is to localise a moving object based on a spatial distribution of transceivers (anchors) using an asynchronous TDoA algorithm. The designed experiment aims to provide the precision and accuracy maps of the position measurements obtained with an IPS. These maps will be used by the subsequently introduced debiasing filter.

The IPS in question, which is depicted in Fig. 1, consists of a drone to be localised and four transceiver anchors positioned at the vertices and facing the centre of a square domain. All the antennae are at a height of 20 cm from the floor. The drone is on a moving stand equipped with a laser pointer, which is aligned with the onboard UWB antenna in order to achieve reference positioning of high precision ($\pm$1mm) and accuracy. The equally spaced markers stuck to be floor are the sampling positions, as shown in Fig. 2.

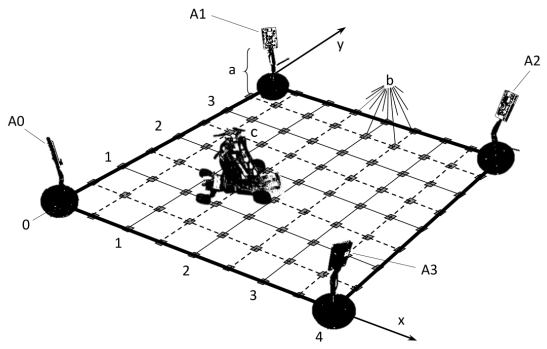

Fig. 1. Diagram of the setup of the studied 4×4 m^2 IPS for 2D localisation: (a) are the adjustable stands of the (A0-A3) transmitting anchors antennae, (b) the measurement points regularly distributed every 50 cm in both directions, and (c) the mobile stand for the object to be localised.

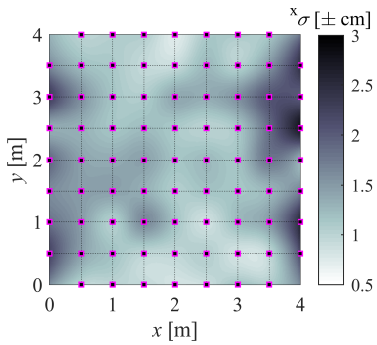

Fig. 2. Precision mapping ($\pm^{x}\sigma$) of the x component of the position. The sampling points are the magenta squares.

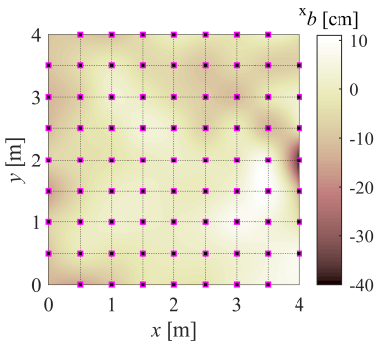

Fig. 3. Accuracy mapping (^{x}b) of the x component of the position. The sampling points are the magenta squares.

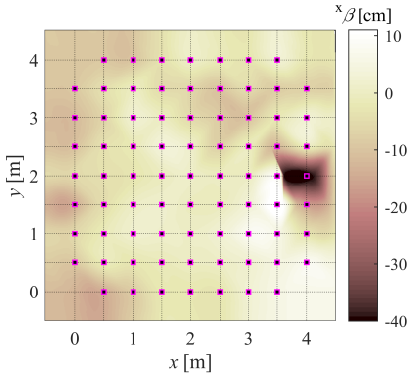

Fig. 4. Debiasing surface ($^{x}\beta$) for the x component obtained by cubic spline interpolation of the estimated scattered debiasing values ($^{x}\beta_{ij}$).

In order to build the maps, a large number of measurements ($N = 700$) are taken at a sampling frequency of 100 Hz while keeping the drone still for at least 30 seconds on each marker (X_{ij}). Then, the raw stream of data is post-processed getting rid of the transients corresponding to the movement between markers. The drone is kept aligned with the x axis and parallel to the floor, as the effect of its direction is not being investigated. Finally, the bias (b), standard deviation (σ) and mean squared error (MSE) are computed. For instance, their values in the x direction (superscript ^{x}) are as follows:

$$\begin{aligned} {}^{x}b_{ij} &= N^{-1}\textstyle\sum_{k=1}^{N} x^{(k)} - X_{ij} \\ {}^{x}\sigma_{ij} &= \left({}^{x}\mathrm{MSE}_{ij} - {}^{x}b_{ij}^{2}\right)^{0.5} \\ {}^{x}\mathrm{MSE}_{ij} &= N^{-1}\textstyle\sum_{k=1}^{N}\left(x^{(k)} - X_{ij}\right)^{2} \end{aligned} \tag{1}$$

where $x^{(k)}$ is the k^{th} position measurement. The resulting maps can be found in Fig. 2 and Fig. 3.

III. Formulation of Debiasing Filter

The objective of the debiasing filter is to correct the raw EKF estimation of the position ($\mathbf{x} = [x, y]^{\mathrm{T}}$) so that the filtered position ($\hat{\mathbf{x}}$) is approximately the same as the actual real position ($\mathbf{X} = [X, Y]^{\mathrm{T}}$). The debiasing filter on the sample points described in Section II should provide the real position.

From the definition of bias and variance in (1), the measurement on a reference point can be factorised into (2): the real position, the bias, and a random fluctuation ($\mathcal{R}$) which is a function of the standard deviation. Note that both b and σ are functions of the real position. For the proposed formulation, $\mathcal{R}$ will be neglected even if this affects the quality of the filter.

$$\begin{aligned} x_{ij} &= X_{ij} + {}^{x}b_{ij} + \cancel{\mathcal{R}({}^{x}\sigma_{ij})} \\ {}^{x}b_{ij} &= {}^{x}b(X_{ij}, Y_{ij}) \\ {}^{x}\sigma_{ij} &= {}^{x}\sigma(X_{ij}, Y_{ij}) \end{aligned} \tag{2}$$

Since the input of the filter is going to be the estimated position, but the bias map in Fig. 3 is a function of the real position, a change of domain is needed. As implicitly suggested by (2), the change of domain is expressed as in (3). In this case, the debiasing value will be simply the raw bias with opposite sign, i.e. ${}^{x}\beta_{ij} = -{}^{x}b_{ij}$.

$$\bar{\mathbf{X}}_{ij} = \mathbf{X}_{ij} + [{}^{x}b_{ij}, {}^{y}b_{ij}]^{\mathrm{T}} \tag{3}$$

Hence, the obtained debiasing values are no longer functions of the real position (which is unknown) but are function of the measured position. As shown in (4) for the x direction, the sampled debiasing discrete distributions β_{ij} in both directions can be interpolated over a deformed grid [$\bar{X}_{ij}$,$\bar{Y}_{ij}$], obtaining debias surfaces that are functions of the measured positions.

$$\begin{bmatrix} \bar{X}_{ij} & \bar{Y}_{ij} & {}^{x}\beta_{ij} \end{bmatrix} \overset{interp.}{\rightarrow} {}^{x}\beta(\mathbf{x}) \tag{4}$$

For instance, in Fig. 4, ${}^{x}\beta(\mathbf{x})$ is described by a simple cubic spline. Since the debiasing filter must be applied in real time, a more efficient interpolation method will be considered in the future. Finally, the debiasing values can be directly added to the measured position obtaining the filtered estimation $\hat{\mathbf{x}}$:

$$\hat{x} = x + {}^{x}\beta(\mathbf{x}) \qquad \hat{y} = y + {}^{y}\beta(\mathbf{x}) \tag{5}$$

IV. Conclusion and Future Work

An experimental evaluation of the distribution of variance and bias of positioning estimations was performed. The precision values are bounded by ±3cm as predicted by a previous theoretical study of IPSs [11]. However, the accuracy level was unsatisfactory. In order to increase it, a data-driven debiasing filter was formulated. The debiasing surface obtained is a function of only the biases measured on a discrete number of points. At present, this work is being extended towards a more comprehensive filtering procedure aimed at increasing both precision and accuracy. The debiasing filter being developed will also consider the variance. In addition, interpolating neural networks will enable three dimensions. The experimental platform will be further improved and employed for tests and validation of these filters. Furthermore, the developed IPS with high precision and accuracy will also be used for indoor experiments to test multi-agent self-coordination and collision-avoidance algorithms – e.g. in [12].

REFERENCES

[1] M. W. Mueller, M. Hamer, and R. D'Andrea, "Fusing ultra-wideband range measurements with accelerometers and rate gyroscopes for quadcopter state estimation," in *International Conference on Robotics and Automation (ICRA)*. IEEE, May 2015.

[2] M. W. Mueller, M. Hehn, and R. D'Andrea, "Covariance correction step for kalman filtering with an attitude," *Journal of Guidance, Control, and Dynamics*, vol. 40, no. 9, pp. 2301–2306, sep 2017.

[3] A. Alarifi, A. Al-Salman, M. Alsaleh, A. Alnafessah, S. Al-Hadhrami, M. Al-Ammar, and H. Al-Khalifa, "Ultra wideband indoor positioning technologies: Analysis and recent advances," *Sensors*, vol. 16, no. 5, p. 707, may 2016.

[4] M. Ghavami, L. Michael, and R. Kohno, *Ultra Wideband Signals and Systems in Communication Engineering*. John Wiley & Sons, 2007.

[5] M. Compagnoni, R. Notari, F. Antonacci, and A. Sarti, "A comprehensive analysis of the geometry of TDOA maps in localization problems," *Inverse Problems*, vol. 30, no. 3, p. 035004, feb 2014.

[6] S. O. Dulman, A. Baggio, P. J. Havinga, and K. G. Langendoen, "A geometrical perspective on localization," in *Proceedings of the first ACM international workshop on Mobile entity localization and tracking in GPS*. ACM Press, 2008.

[7] M. Compagnoni and R. Notari, "Tdoa-based localization in two dimensions: the bifurcation curve," *Fundamenta Informaticae*, vol. 135, no. 1-2, pp. 199–210, 2014.

[8] R. Kaune, J. Horst, and W. Koch, "Accuracy analysis for tdoa localization in sensor networks," in *14th International Conference on Information Fusion*, 2011.

[9] R. Kaune, "Accuracy studies for tdoa and toa localization," Aug. 2012.

[10] M. Compagnoni, A. Pini, A. Canclini, P. Bestagini, F. Antonacci, S. Tubaro, and A. Sarti, "A geometrical–statistical approach to outlier removal for TDOA measurements," *IEEE Transactions on Signal Processing*, vol. 65, no. 15, pp. 3960–3975, aug 2017.

[11] P. Grasso and M. S. Innocente, "Theoretical study of signal and geometrical properties of two-dimensional uwb-based indoor positioning systems using tdoa," in *6th International Conference on Mechatronics and Robotics Engineering (ICMRE)*. IEEE, Feb. 2020.

[12] M. S. Innocente and P. Grasso, "Self-organising swarms of firefighting drones: Harnessing the power of collective intelligence in decentralised multi-robot systems," *Journal of Computational Science*, vol. 34, pp. 80–101, may 2019.